

# A Complete Representation of Structure-Property Relationships in Crystals

A. van de Walle<sup>1</sup>

<sup>1</sup>*Engineering and Applied Science Division,*

*California Institute of Technology, Pasadena, California 91125, USA*

While structure-property relationships have long guided the discovery and optimization of novel materials,<sup>1–3</sup> formal quantitative methods to identify such relationships in crystalline systems are beginning to emerge.<sup>4–8</sup> Among them is the cluster expansion<sup>9–13</sup> (CE), which has been successfully used to parametrize the configurational dependence of important scalar physical properties such as band gaps,<sup>14</sup> Currie temperatures,<sup>15</sup> equation of state parameters,<sup>16,17</sup> and densities of states.<sup>18–20</sup> However, the CE is currently unable to handle anisotropic properties, a key distinguishing feature of crystalline systems central to the design of modern epitaxial structures and devices. Here we introduce the tensorial cluster expansion (TCE) enabling the prediction of fundamental tensor-valued material property such as elasticity, piezoelectricity, dielectric constants, optoelectric coupling, anisotropic diffusion coefficients, surface energy and stress, etc. As an application, we develop predictive ab initio models of anisotropic properties relevant to the design and optimization of III-V semiconductor epitaxial optoelectronic devices.<sup>21,22</sup>

As in a conventional CE, we represent an atomic *configuration*  $\sigma$  by a vector of all occupation variables  $\sigma_i$  indicating which type of atom resides on lattice site  $i$ . In a binary alloy, the two possible chemical species are conventionally assigned the values  $\sigma_i = \pm 1$ , in analogy with the well-known Ising model (an extension to multicomponent alloys is straightforward<sup>9</sup>). The conventional CE formalism establishes that polynomials of these occupation variables  $\sigma_i$  form a complete orthogonal basis (i.e. any scalar function of configuration can be expressed as such).

We now construct a TCE by forming a so-called *tensor product* of (i) this polynomial basis with (ii) an orthogonal basis for the tensor of interest (e.g., a basis consisting of all tensors containing a single nonzero entry). In other words, every possible pairwise combination of one term of (i) with one term of (ii) is considered as a potential term of the TCE. Next, symmetry considerations are used to eliminate terms that must vanish by symmetry and identify coefficients that must be identical by symmetry. The resulting TCE of the configurational dependence of a property  $Q(\sigma)$  has the general form (see Supplementary Discussion 1 for a proof)

$$Q(\sigma) = \sum_{\alpha} \sum_{\beta \in C(\alpha)} J_{\alpha\beta} m_{\alpha\beta} \left\langle \beta' \prod_{i \in \alpha'} \sigma_i \right\rangle_{(\alpha, \beta)} \quad (1)$$

where  $\alpha$  is a *cluster* (i.e. a set of lattice sites). The outer sum is over all possible clusters  $\alpha$  that are mutually symmetrically distinct under the space group of the underlying lattice. The inner sum is over all basis tensors  $\beta$  in the set  $C(\alpha)$  of basis tensors that are compatible with the subgroup of symmetry operations that map cluster  $\alpha$  onto itself. The average  $\langle \dots \rangle_{(\alpha, \beta)}$  is over all clusters-tensor pairs  $(\alpha', \beta')$  that are equivalent by symmetry to the clusters-tensor pair  $(\alpha, \beta)$ . The coefficients  $m_{\alpha\beta}$  are multiplicities indicating the number of clusters-tensor pairs  $(\alpha', \beta')$  equivalent to  $(\alpha, \beta)$  by symmetry (e.g. per unit cell).

While the quantities introduced so far only depends on the geometry of the lattice and the rank of the tensor considered, the coefficients  $J_{\alpha\beta}$  encode a specific structure-property relationship  $Q(\sigma)$  between the configuration  $\sigma$  and the tensor  $Q$  of interest. They can be determined from a least-squares fit to a “training” database of quantum mechanical calculations<sup>14</sup> of the property  $Q$  for various configurations  $\sigma$ . Once the  $J_{\alpha\beta}$  are known, the property of interest can be predicted, in a computationally efficient way, for compounds not included in the training database. In addition, each term in the sum (1) provides individual geometric insight regarding a possible coupling between structure and property (as illustrated in Fig. 1), the strength of which is determined by the coefficient  $J_{\alpha\beta}$  multiplying each term.

The proposed TCE formalism fully generalizes two existing and widely-used principles: (i) the property tensors symmetry restrictions in crystals<sup>23</sup> (obtained by re-

ducing the outer sum in (1) to a single term corresponding to the “empty” cluster) and (ii) the traditional CE (obtained by reducing the inner sum in (1) to a single term corresponding to  $\beta = 1$ ). It also generalizes a recently proposed CE scheme limited to tensorial properties of fully disordered alloys.<sup>24</sup>

Unlike in a scalar CE, each cluster may introduce multiple terms in the TCE, namely, one for each symmetrically distinct contributions to the tensor of interest. As a simple example, in a TCE of elastic constants in a cubic system, the empty cluster yields separate contributions to the  $C_{11}$ ,  $C_{12}$  and  $C_{44}$  elastic constants, reflecting the fact that cubic symmetry does not impose any relationships among these elastic constants, while all remaining elastic constants are uniquely determined once these three are fixed. Other clusters will typically yield even more independent contributions, reflecting the fact that each cluster exhibits a local point symmetry no larger than the symmetry of the crystal as a whole.

A TCE cannot be constructed by merely building a separate scalar CE for each element of the tensor of interest. For instance, the  $C_{11}$  elastic constant in an ordered fcc alloy is affected differently by a second nearest neighbor (2nn) pair along the  $x$  or the  $y$  axis, because the unique direction ( $x$ ) associated with that elastic constant effectively breaks the cubic symmetry of the underlying lattice. A scalar CE would incorrectly assign the same coupling between  $C_{11}$  and these two clusters. Moreover, a separate CE for each elastic constant would fail to exploit the fact that the coupling between  $C_{11}$  and a pair along  $y$  is the same as the coupling between  $C_{22}$  and a pair along  $z$ , resulting in a large and unnecessary increase in the number of parameters in the CE and a corresponding increase in the size of database required to fit them.

When *all* clusters terms in the TCE are included in the sum (1), *any* function  $Q(\sigma)$  of configuration can be represented by an appropriate selection of the values of  $J_{\alpha\beta}$ . The crux of the argument leading to that conclusion lies in establishing that the term in brackets in (1) forms an orthogonal basis for the space of tensor functions of configurations. A TCE proves especially useful when a *truncated* TCE is found to converge rapidly with respect to the number of terms included in the sum. A good accuracy can often be achieved by keeping only clusters  $\alpha$  that are relatively compact (*e.g.* short-range pairs or small triplets).<sup>9,10,12,13,25</sup> The selection of the most important clusters (*i.e.* those explaining most of the changes in  $Q(\sigma)$ ) can be carried out automatically via cross-validation error minimization.<sup>26</sup>

Our approach enables the exploration of the properties of arbitrary superstructures of a given primitive unit cell, a capability particularly well-adapted, for instance, to the design and optimization of epitaxial superlattices of III-V semiconductors. Modern molecular beam epitaxy or metallo-organic chemical vapor deposition techniques offer remarkable control over the atomic configuration in this class of systems. For

instance, superlattice structures can be readily deposited with atomic monolayer accuracy and by selecting suitable substrate orientations, various superlattice orientations can be achieved. The TCE proves useful in this context because it is far less time-consuming to explore the properties of potential superlattices via a TCE than via purely experimental techniques.

As an illustration, we have constructed TCEs of the configurational dependence of the static strain tensor (relative to a reference equiatomic random alloy), the strain-dependence of the band gap, the elastic constant tensor and the piezoelectric tensor for the wurtzite  $\text{Ga}_x\text{In}_{1-x}\text{N}$  semiconductor system. These TCEs are based upon a least-squares fit to a database ab initio calculations (as described in the Methods Summary) and are represented in Fig. 2. Each TCE includes the “empty” cluster, the point cluster and the two distinct nearest neighbor pair clusters (labelled “a” and “b”), which had the largest effect on the properties studied. The inclusion of longer ranged pairs and multibody clusters was attempted but did not yield any improvement in the cross-validation error. The configurational-dependence of static strain and the one of strain-gap coupling shown in Fig. 2 are the sum of all corresponding pair contributions depicted in Fig. 1, each weighted by the corresponding coefficients  $J_{\alpha\beta}$  reported in Table 1. Similar data for the elastic and piezoelectric constants are provided in the Supplementary Discussion 2.

We now provide a few instructive examples of the type of information that can be extracted from such structure-property relationships. The calculated configurational-dependence of static strain enables us to conclude that, if a uniaxial tensile strain were imposed along the  $\langle 10\bar{1}0 \rangle$  direction (e.g. by using a suitably lattice-mismatched substrate or by bending the substrate), the crystal’s thermodynamically stable structure would be directed towards the formation of ordered layers along  $\langle 10\bar{1}0 \rangle$ . (The ordering would take place after suitable annealing and may take the form of short-range order at low strains.) This finding is useful for two independent reasons: (i) it depresses the unwanted tendency of  $\text{Ga}_x\text{In}_{1-x}\text{N}$  to phase separate and (ii) it offers an avenue to induce superlattices perpendicular to the growth direction (assuming a (0001) substrate).

The dependence of the band gap on strain could be exploited to devise tunable optoelectronic devices. Our calculated configurational-dependence of this quantity indicates that ordering along the  $\langle 0001 \rangle$  direction would maximize the strain-gap coupling and that uniaxial strain would maximize the effect (for otherwise there would be cancellations of the positive and negative effects along orthogonal directions under biaxial strain). This effect occurs almost exclusively through the pair clusters of type “b” (lying in the (0001) plane).

The configurational-dependence of the elastic constant is found to be weak (relative

to the magnitude of the elastic constants in this system, i.e., a few hundred GPa), but exhibits the interesting feature that the largest effects are not along the directions that simple geometric intuition would suggest, thus illustrating the necessity to carry out full quantum mechanical calculations. In other systems, where this coupling could be larger, this type of calculation would yield the identification of atomic ordering inducing elastically soft directions enabling coherent depositions under a wider range of lattice mismatch.

The configurational-dependence of the piezoelectric constants is more complex. For conciseness, we focus on the electric dipole along the  $\langle 0001 \rangle$  axis only (the configurational-dependence of the full piezoelectric tensor is given in the Supplementary Discussion 2). As intuitively expected, the direction of uniaxial strain that couples the most strongly with a dipole along the  $\langle 0001 \rangle$  axis through type “a” pairs is about  $45^\circ$  off the axis of the pair. Strain along such an axis would induce the largest rotation of the pair and cause the neighboring N-(Ga,In) dipole to align more along the  $\langle 0001 \rangle$  axis. In contrast, the stronger coupling via type “b” pairs which are perpendicular to the  $\langle 0001 \rangle$  direction is unexpected and reveals that ordering along the  $\langle 10\bar{1}0 \rangle$  direction could have significant impacts on the piezoelectric response, again illustrating the benefits of a rigorous method to extract structure-property relationships from quantum mechanical calculations over simple geometric intuition.

Structure-property relationships may sometimes involve long-range coupling that cannot accurately be represented by a short-range cluster-expansion. A classical example of this issue is the persistence of the orientation-dependence of the coherency strain energy of superlattice structures even in the long-period limit<sup>25</sup>. A natural way to handle this issue is to add, to the short-range cluster expansion, explicit long-range decaying interactions with a pre-specified, but flexible, behavior. For instance, long-range pair interactions  $J_{\alpha\beta}$  can be represented in the form

$$S(|r|) \left( \sum_m R_1^m Y^m(\theta, \phi) |r|^{-1} + \sum_m R_2^m Y^m(\theta, \phi) |r|^{-2} + \dots \right)$$

where  $r$  is the distance between the two sites in the pair and  $(\theta, \phi)$  describes the pair’s orientation. The rate of decay  $r^{-k}$  of these interactions covers the wide majority of field-mediated long-range interactions (e.g. electrostatic or elastic). Depending on the number of terms included, this series can exactly represent interactions due to, monopole-monopole, dipole-monopole, etc. The direction dependence is modeled via “harmonics”  $Y^m(\theta, \phi)$  adapted to the symmetry of the lattice. These harmonics can be generated using an algorithm similar to the construction of the “empty cluster” term of a TCE, by exploiting the fact that any function of direction can be represented as a polynomial expansion in terms of the elements of a unit directional

vector. The coefficients in this polynomial can be represented by tensors obeying the same symmetry transformation rules as those used in a TCE. The coefficients  $R_j^m$ , representing the strength of the coupling, are to be determined via a least-squares fit. The prefactor  $S(|r|)$  is a function such that  $|r|^{-k} S(|r|) \rightarrow 0$  as  $|r| \rightarrow 0$  for the positive integers  $k$  considered, in order to eliminate the divergences at the origin and let the short-range cluster expansion govern the short-range coupling. An alternative approach to handle infinite-range coupling is to express pairwise interactions in reciprocal space.<sup>25</sup>

Our general method to construct structure-property relationships in crystals via a TCE could be used in a number of other contexts. For instance, it could encode the coupling between order parameters and elastic constants in phase field modeling<sup>2,27</sup> or enable computationally efficient combinational searches<sup>15</sup> for configurations exhibiting desirable properties. More generally, it will provide insight regarding how properties can be optimized in the large class of materials taking the form of crystals. To this effect, the software tools developed for this work have been incorporated in the Alloy Theoretic Automated Toolkit (ATAT), a freely distributed software package available at <http://alum.mit.edu/www/avdw/atat>. This implementation covers all space groups as well as multicomponent and multi-sublattice systems. In addition, its object-oriented structure facilitates extensions to any other object with well-defined symmetry transformation rules (e.g. tensor fields or parametrized families of tensors).

## Methods

The quantum mechanical calculations based on the Density Functional Theory formalism were performed using the VASP package<sup>28,29</sup> using the projector augmented wave method.<sup>30</sup> The standard library potentials “N”, “Ga” and “In” were used and the following settings were employed: A plane wave energy cutoff of 500 eV, a  $k$ -point mesh of at least  $1536/n$  points in the Brillouin zone (where  $n$  is the number of atoms in the unit cell) and the exchange-correlation functional was set to PW91. The proper piezoelectric constants were calculated using Berry phase method implemented in the VASP package<sup>31</sup>.

All strain derivatives (elastic and piezoelectric constants, gap strain-dependence) were obtained via finite differences with respect to imposed strains of 0.5% and -0.5% along the minimum number of distinct modes given the symmetry of each superstructure considered.

The TCEs were calculated using a training database of 94 superstructures of the primitive wurtzite lattice (except for the piezoelectric TCE, which was based upon 24

superstructures). The optimal number of terms in the TCE was determined via cross-validation while the choice of the superstructures to be included in the least-square fit of the TCE was based upon a variance minimization criterion.<sup>26</sup>

---

- <sup>1</sup> Olson, G. Computational design of hierarchically structured materials. *Science* **277**, 1237–1242 (1997).
- <sup>2</sup> Liu, Z. K., Chen, L. Q., and Rajan, K. Linking length scales via materials informatics. *JOM* **58**, 42–50 (2006).
- <sup>3</sup> Ashby, M. F. *Materials Selection in Mechanical Design*. Butterworth-Heinemann, Oxford, second edition, (1999).
- <sup>4</sup> Morgan, D., Ceder, G. and Curtarolo, S. High-throughput and data mining with ab-initio methods. *Meas. Sci. & Tech.* **16**, 296–301 (2005).
- <sup>5</sup> Morgan, D. and Ceder, G. Data mining in materials development. In *Handbook of Materials Modeling*, Yip, S., editor, volume Part A, 395–422. Springer, Dordrecht, the Netherlands (2005).
- <sup>6</sup> Suh, C. and Rajan, K. Virtual screening and qsar formulations for crystal chemistry. *QSAR and Combinational Science* **24**, 114–119 (2005).
- <sup>7</sup> Johannesson, G. H. et al. Combined electronic structure and evolutionary search approach to materials design. *Phys. Rev. Lett.* **88**, 255506 (2002).
- <sup>8</sup> Rajan, K. Materials informatics. *Materials Today* **8**, 38–45 (2005).
- <sup>9</sup> Sanchez, J. M., Ducastelle, F., and Gratias, D. Generalized cluster description of multicomponent systems. *Physica* **128A**, 334–350 (1984).
- <sup>10</sup> de Fontaine, D. Cluster approach to order-disorder transformation in alloys. *Solid State Phys.* **47**, 33–176 (1994).
- <sup>11</sup> Zunger, A. First principles statistical mechanics of semiconductor alloys and intermetallic compounds. In *NATO ASI on Statics and Dynamics of Alloy Phase Transformation*, Turchi, P. E. and Gonis, A., editors, volume 319, 361–419 (Plenum Press, New York, 1994).

- <sup>12</sup> Asta, M., Ozolins, V., and Woodward, C. A first-principles approach to modeling alloy phase equilibria. *JOM - Journal of the Minerals Metals & Materials Society* **53**, 16–19 (2001).
- <sup>13</sup> Ceder, G., van der Ven, A., Marianetti, C., and Morgan, D. First-principles alloy theory in oxides. *Modelling Simul. Mater Sci Eng.* **8**, 311–321 (2000).
- <sup>14</sup> Franceschetti, A. and Zunger, A. The inverse band-structure problem of finding an atomic configuration with given electronic properties. *Nature* **402**, 60–63 (1999).
- <sup>15</sup> Franceschetti, A., Dudiy, S. V., Barabash, S. V., Zunger, A., Xu, J., and van Schilfgaarde, M. First-principles combinatorial design of transition temperatures in multicomponent systems: The case of Mn in GaAs. *Phys. Rev. Lett.* **97**, 047202 (2006).
- <sup>16</sup> Asta, M., McCormack, R., and de Fontaine, D. Theoretical study of alloy stability in the Cd-Mg system. *Phys. Rev. B* **48**(2), 748–766 (1993).
- <sup>17</sup> Geng, H. Y., Sluiter, M. H. F., and Chen, N. X. Order-disorder effects on the equation of state for fcc Ni-Al alloys. *Phys. Rev. B* **72**, 014204 (2005).
- <sup>18</sup> Garbulsky, G. D. and Ceder, G. Effect of lattice vibrations on the ordering tendencies in substitutional binary alloys. *Phys. Rev. B* **49**, 6327–6330 (1994).
- <sup>19</sup> Geng, H. Y., Sluiter, M. H. F., and Chen, N. X. Cluster expansion of electronic excitations: Application to fcc Ni-Al alloys. *Journal of Chemical Physics* **122**, 214706 (2005).
- <sup>20</sup> van de Walle, A. and Ceder, G. The effect of lattice vibrations on substitutional alloy thermodynamics. *Rev. Mod. Phys.* **74**, 11–45 (2002).
- <sup>21</sup> Pearton, S. J., Zolper, J. C., Shul, R. J., and Ren, F. GaN: Processing, defects, and devices. *J. Appl. Phys.* **86**, 1–78 (1999).
- <sup>22</sup> Ambacher, O. Growth and applications of group III-nitrides. *J. Phys. D* **31**, 2653–2710 (1998).
- <sup>23</sup> Nye, J. F. *Physical Properties of Crystals: Their Representation by Tensors and Matrices*. Oxford University Press, USA, (1985).
- <sup>24</sup> Liu, J. Z., van de Walle, A., Ghosh, G., and Asta, M. Structure, energetics, and me-

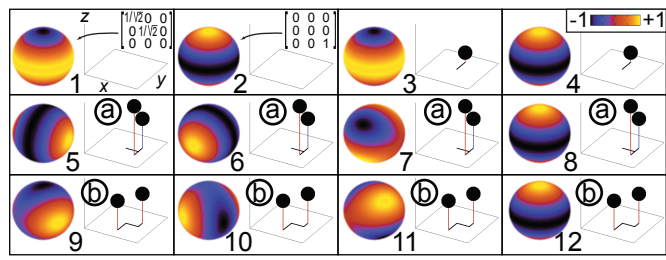
- chanical stability of Fe-Cu bcc alloys from first-principles calculations. *Phys. Rev. B* **72**, 144109 (2005).
- <sup>25</sup> Laks, D. B., Ferreira, L. G., Froyen, S., and Zunger, A. Efficient cluster expansion for substitutional systems. *Physical Review B* **46**, 12587–12605 (1992).
- <sup>26</sup> van de Walle, A. and Ceder, G. Automating first-principles phase diagram calculations. *Journal of Phase Equilibria* **23**, 348–359 (2002).
- <sup>27</sup> Lund, A. and Voorhees, P. W. The effects of elastic stress on coarsening in the Ni-Al system. *Acta Materialia* **50**, 2085–2098 (2002).
- <sup>28</sup> Kresse, G. and Furthmüller, J. Efficient iterative schemes for ab initio total-energy calculations using a plane-wave basis set. *Phys. Rev. B* **54**, 11169–11186 (1996).
- <sup>29</sup> Kresse, G. and Furthmüller, J. Efficiency of ab-initio total energy calculations for metals and semiconductors using a plane-wave basis set. *Comput. Mater. Sci.* **6**, 15–50 (1996).
- <sup>30</sup> Kresse, G. and Joubert, D. From ultrasoft pseudopotentials to the projector augmented-wave method. *Phys. Rev. B* **59**, 1758–1775 (1999).
- <sup>31</sup> Vanderbilt, D. and King-Smith, R. D. Electronic polarization in the ultrasoft pseudopotential formalism. Unpublished report, (1998).

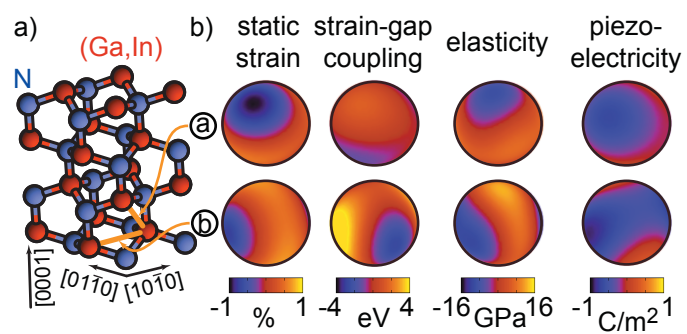
**Acknowledgements** This research was supported by the US National Science Foundation through TeraGrid resources provided by NCSA and SDSC under grant DMR060011N and through the Center for the Science and Engineering of Materials at Caltech.

**Fig 1 Legend:** Graphical representation of each term of the TCE on the cation sublattice of the wurtzite structure expressing the configurational dependence of a symmetric rank two tensor. Each numbered box is associated with a pair  $(\alpha, \beta)$  and corresponding term in Equation (1). Each left panel represents the tensor  $\beta_{i_1, \dots, i_k}$  by plotting the function  $f(u) = \sum_{i_1, \dots, i_k} \beta_{i_1, \dots, i_k} u_{i_1} \cdots u_{i_k}$  for all values of the vector  $u$  on the unit sphere (for illustrative purposes, the two tensors  $\beta_{i_1, \dots, i_k}$  associated with the “empty” cluster are also reported in cartesian coordinates). Each right panel represents the cluster  $\alpha$  (only the cation sites are shown, not the anions). Here, the “empty”, point and the two distinct nearest neighbor pair clusters (labelled “a” and “b”) are enumerated. Each cluster is repeated in more than one box, because a cluster can separately couple with multiple elements of the tensor.

**Fig. 2 Legend:** Structure-property relationships. a) Wurtzite structure of  $\text{Ga}_x\text{In}_{1-x}\text{N}$  in which the two symmetrically distinct nearest-neighbor pairs of  $(\text{Ga}, \text{In})$  sites, having the largest effect of the properties studied, are marked in orange and labelled “a” and “b”. b) Each color-coded sphere represents the total change in the contribution of each pair cluster to the tensor of interest when a pair of unlike atoms is replaced by a pair of alike atoms (using the same graphical device as in Fig 1). The calculated structure-property relationships also contain constant and composition-dependent terms (not shown). The piezoelectric plot depicts the coupling between the  $\langle 0001 \rangle$  component of the electric dipole with the full strain tensor.

**Table 1 Legend: Coefficients of the TCE of Static Strain and Strain-Gap Coupling.**





Cluster-tensor (index in Fig. 1)	Term in TCE (in Fig. 2)	$m_{\alpha\beta}$	Static Strain			Strain-Gap Coupling		
			Coefficient	Standard	$J_{\alpha\beta}$ (%)	error	Coefficient	Standard
1	-	1			2.52	0.02	-4.03	0.14
2	-	1			0.78	0.02	-6.33	0.14
3	-	2			7.88	0.04	3.08	0.34
4	-	2			5.03	0.04	6.31	0.34
5	a	6			0.15	0.02	-0.08	0.14
6	a	6			0.03	0.02	-0.13	0.14
7	a	6			0.49	0.02	-0.93	0.22
8	a	6			-0.24	0.01	0.30	0.11
9	b	6			0.16	0.01	-0.45	0.10
10	b	6			-0.45	0.01	2.84	0.11
11	b	6			-0.07	0.05	0.30	0.43
12	b	6			0.31	0.01	0.54	0.10